Biophysical Letter

Retinal Flip in Rhodopsin Activation?

Jun Feng,[1] Michael F. Brown,[2,3] and Blake Mertz[1,*]
[1]The C. Eugene Bennett Department of Chemistry, West Virginia University, Morgantown, West Virginia; [2]Department of Chemistry and Biochemistry and [3]Department of Physics, University of Arizona, Tucson, Arizona

ABSTRACT Rhodopsin is a well-characterized structural model of a G protein-coupled receptor. Photoisomerization of the covalently bound retinal triggers activation. Surprisingly, the x-ray crystal structure of the active Meta-II state has a 180° rotation about the long-axis of the retinal polyene chain. Unbiased microsecond-timescale all-atom molecular dynamics simulations show that the retinal cofactor can flip back to the orientation observed in the inactive state of rhodopsin under conditions favoring the Meta-I state. Our results provide, to our knowledge, the first evidence from molecular dynamics simulations showing how rotation of the retinal ligand within its binding pocket can occur in the activation mechanism of rhodopsin.

Received for publication 2 March 2015 and in final form 9 April 2015.

*Correspondence: blake.mertz@mail.wvu.edu

Understanding the specific intermolecular interactions that lead to G protein-coupled receptor (GPCR) function is one of the most pressing needs in the design of targeted chemotherapeutics. Rhodopsin, a prototypical GPCR, is activated when its covalently bound chromophore, retinal, absorbs a photon and undergoes an 11-*cis* → all-*trans* isomerization, culminating in an equilibrium between inactive Meta-I and active Meta-II forms (Fig. 1, *a–c* and Fig. S1 in the Supporting Material) (1). Most NMR spectroscopic and crystallographic structures of various photointermediates reveal the retinal ligand acting as an inverse agonist (2–5). However, recent x-ray structures of the active Meta-II state are very surprising, in that retinal is rotated 180° about its long axis versus inactive photointermediates (6,7). This has led to uncertainty as to the role of the retinal orientation: does the polyene chain undergo a long-axis rotation in the transition from Meta-I to Meta-II—and if so, what is the biological relevance of this striking large-scale movement?

We used unbiased μs-timescale, all-atom molecular dynamics (MD) simulations of rhodopsin in a series of lipid bilayers, taking advantage of the microscopic reversibility of the Meta-I to Meta-II transition to investigate the behavior of the retinal orientation. Our results clearly show that upon photoactivation retinal possesses remarkable flexibility: we present what is, to our knowledge, the first theoretical evidence of a long-axis flip of the retinal cofactor in the rhodopsin activation process. In two of three simulations, long-axis rotation of the retinal polyene chain was clearly observed, leading to a reorientation toward the extracellular side of the protein. These results create an important bridge between spectroscopic and crystallographic studies (1,3). Furthermore, these results provide evidence for a loose coupling between agonist and receptor upon GPCR activation, as suggested from experimental and computational studies (1,8,9).

We utilized the fact that the lipid bilayer composition can significantly influence the Meta-I to Meta-II equilibrium (1,10). Our hypothesis was that long-axis rotation of the polyene chain occurs in Meta-II due to an ensemble of activated conformations that all possess a larger binding pocket than inactive forms of rhodopsin. To test this hypothesis, we modeled the Meta-II structure of rhodopsin under Meta-I protonation states embedded in a bilayer of lipids known to forward- or back-shift the Meta-I to Meta-II equilibrium using μs-long all-atom MD simulations (1) (for details, see the Supporting Material). Meta-II conformations are defined by the state of two protonation switches involving the protonated Schiff base (SB) with its complex counterion, as well as Glu134$^{3.49}$ (superscript denotes Ballesteros-Weinstein numbering) of the conserved E(D)RY motif (1). Furthermore, the reversible transition to an inactive conformation initially requires the polyene chain to rotate with the C9- and C13-methyl groups pointing toward extracellular loop-2 (EL2) as in the dark and Meta-I states.

All-atom MD simulations have proven invaluable to the characterization of the structure-function relationship in rhodopsin activation. In particular, MD studies on the μs-timescale have reproduced solid-state ^{2}H NMR spectra of the Meta-I state (11), and showed an increase in both hydration and retinal flexibility versus the dark state (12). In this study, the most remarkable event occurs at roughly 2.5 μs in two of the three Meta-II to Meta-I simulations: the polyene chain in retinal undergoes a 180° rotation about its long axis, in which the C9- and C13-methyl groups shift

Editor: Scott Feller.

http://dx.doi.org/10.1016/j.bpj.2015.04.040

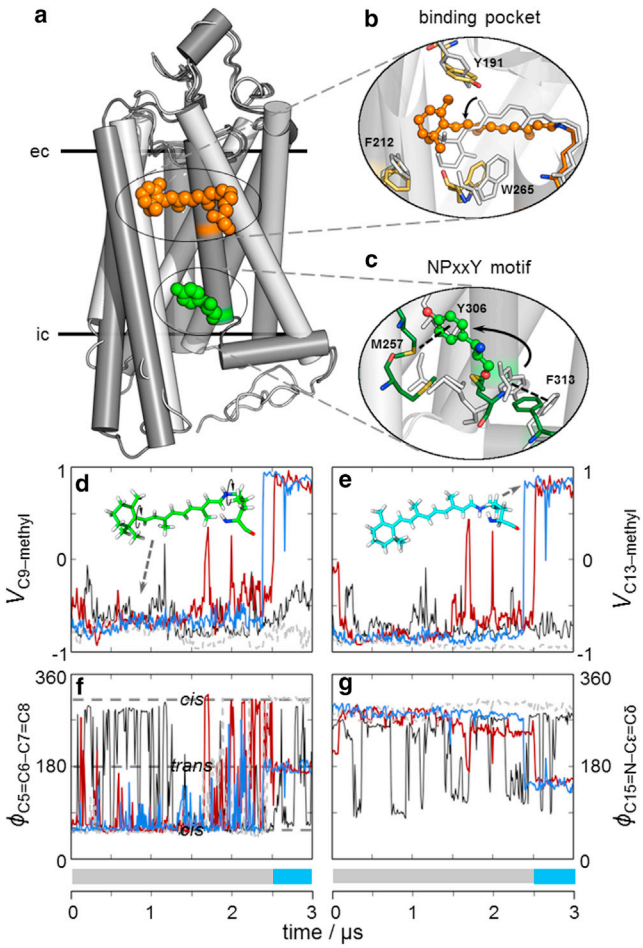

FIGURE 1 Microsecond timescales are required for retinal flip in rhodopsin. (*a*) Retinal undergoes an 11-*cis* to all-*trans* isomerization upon photon absorption, initiating large-scale conformational changes in rhodopsin (*dark gray*, dark state (PDB:1U19); *light gray*, Meta-II-like (PDB:3PXO)). An outward tilt and elongation of TM5 and outward rotation of TM6 are conserved in Class A GPCRs. (*b*) A 180° rotation occurs about the long axis of the retinylidene chain in Meta-II, changing the orientation of the C9- and C13-methyl groups from the extracellular (*ec*) (*gray*) to the cytoplasmic (*ic*) side (*orange*) of the protein. (*c*) Conserved residue Tyr306$^{7.53}$ of the NPxxY motif toggles between π-π interactions with Phe313$^{7.60}$ (dark) and Met257$^{6.40}$ (Meta-II) (*gray*, dark; *green*, Meta-II). (*d–g*) MD trajectories for rhodopsin in various lipid bilayers (*black*, Meta-II; *blue*, DOPC/ DOPE (3:1); *gray*, DOPC/DOPE (1:1); and *red*, DOPC/DOPE (1:3)). (*d*) The C9-CH_3 and (*e*) C13-CH_3 bond orientational time evolution V_t defined as the cosine angle of the bond vector with respect to the membrane normal. At ~2.5 μs, the retinylidene moiety undergoes a long-axis 180° rotation in two trajectories. (*Insets*) Retinal cofactor before (*d*) and after (*e*) the flip. The C5=C6–C7=C8 dihedral (*f*) and the C15–NZ–C_ε–C_δ dihedral (*g*) limit rotation to the polyene chain; the β-ionone ring undergoes a 6-s-*cis* to *trans* conformational transition. To see this figure in color, go online.

orientation from the cytoplasmic side toward the extracellular side of rhodopsin (Fig. 1, *d* and *e*). Once the reorientation occurs, the retinal polyene chain remains stable for the final 500 ns of the simulation. The rotation is notable because our simulations are unbiased, and our control simulation with Meta-II protonation states showed no rotation of the polyene chain. The long-axis rotation is directly related to the dihedral fluctuations that connect both ends of the chromophore, i.e., the β-ionone ring and the retinylidene SB linkage. In particular, the distribution of the dihedral angle for the C6–C7 bond connecting the β-ionone ring to the polyene chain correlates well with previous studies that identified three minima for retinal with a protonated SB (Figs. 1, *f* and *g*, and S2) (13). The final orientation of the β-ionone ring is the 6-*s*-*trans* conformation, a local minimum for the C5=C6–C7=C8 dihedral. The β-ionone ring remains essentially fixed during the polyene chain rotation, with a transition from 6-*s*-*cis* in the starting structure to 6-*s*-*trans*. It has been shown that the 6-*s*-*trans* conformation raises the pK_a of the SB, favoring the protonated state (13), as in Meta-I. Moreover, the pathway that occurs from *cis* to *trans* is very similar to the one observed in previous long-timescale MD studies that examined the dark → Meta-I transition (11,12).

Hydration plays a crucial role in rhodopsin function, in which water is necessary for rearrangement of the chromophore (12,14). The retinal flip is accompanied by a decrease in hydration of the binding pocket (Fig. 2 *a*). Expulsion of water through switching to a Meta-I-like orientation stems from efficient packing between the side chains within the binding pocket and the methyl groups of the retinal (Fig. 2, *b* and *c*). The C9-methyl is directly coupled to the protonation switch of Glu134$^{3.49}$ in fully activated rhodopsin. Removal of the C9-methyl back-shifts rhodopsin to the preactive Meta-I state (15). The back-rotation of the polyene chain reestablishes these interactions, in particular between the C9-methyl and Tyr191^{EL2}. In addition to these interactions, the CWxP motif is part of a transmission switch that is common to many Class A GPCRs, which involves a rotation of Trp265$^{6.48}$ and Phe212$^{5.47}$ that facilitates the outward rotation of TM6 from the inactive to the active state (16). Both flipping events were promptly followed by rotation of Trp265$^{6.48}$ around its χ_1 dihedral, leading to a rearrangement of the indole ring to maintain stabilizing interactions with the retinal (Fig. 2 *d*). Another microdomain critical to GPCR activation involves the conserved NPxxY motif, where Tyr306$^{7.53}$ toggles between aromatic stacking with Phe313$^{7.60}$ in the inactive state and participating in a water-mediated hydrogen-bonding network with Met257$^{6.40}$ in the active state. Both the Tyr306$^{7.53}$–Phe313$^{7.60}$ and Tyr306$^{7.53}$–Met257$^{6.40}$ interactions occur in our simulations, with no correlation to the flip. Although in the Meta-II state Tyr306$^{7.53}$ interacts with Met257$^{6.40}$, this coupling disrupts a staggered interaction among Met253$^{6.36}$, Met257$^{6.40}$, and Met309$^{7.56}$ that is present in the dark state. After ~0.5 μs in two simulations, Tyr306$^{7.53}$ rotates outward to reestablish a π-π stacking interaction with Phe313$^{7.60}$ (Fig. S3, *a–d*). This outward rotation also allows the three methionine side chains to

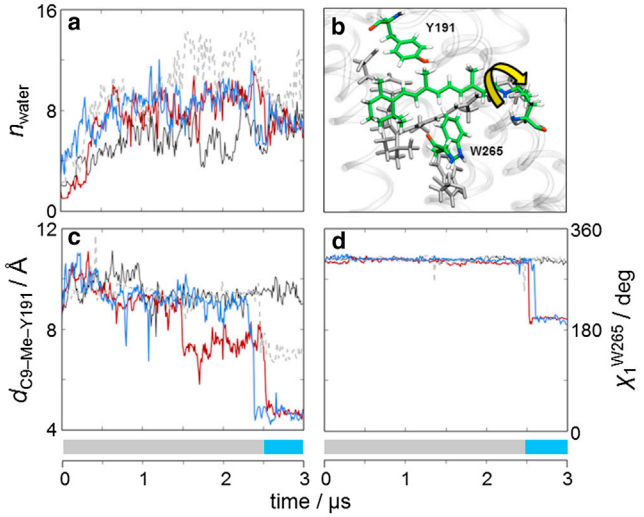

FIGURE 2 Retinal polyene flip is linked to changes in binding pocket hydration and conserved GPCR motifs. (*a*) Back-flip of the retinal polyene chain leads to an expulsion of water from the binding pocket (*black*, Meta-II; *blue*, DOPC/DOPE (3:1); *gray*, DOPC/DOPE (1:1); and *red*, DOPC/DOPE (1:3)). (*b*) Visualization of the retinal binding pocket before and after the flip from the DOPC/DOPE (3:1) trajectory. (*c*) Nonbonded interactions between the C9-methyl and Tyr191^{EL2} are reestablished after the polyene chain flip. (*d*) Rotation of Trp265$^{6.48}$ in the CWxY motif is correlated with the retinal flip. To see this figure in color, go online.

reform the staggered interactions present in the dark state (Fig. S3 *e*).

The flip about the polyene long axis was an unanticipated result from our attempt to model the deactivation of rhodopsin. Interestingly, however, it provides essential insights into the dynamics of the retinal binding pocket (7). The Meta-II structure was obtained from opsin crystals soaked with all-*trans* retinal (7), and this characterization was later supported by a structure of a constitutively active rhodopsin (6). However, comparisons between the Meta-II crystal structure and solid-state NMR studies of frozen detergent-solubilized rhodopsin in the Meta-II state (17) reveal several discrepancies. If one assumes that trapping of the Meta-II photointermediate was equivalent in both NMR and crystallography, then the orientation of retinal in the NMR studies represents an average of those in equilibrium. By starting from the crystal structure and observing a stable 180° rotation about the long axis of the polyene chain, our simulations provide a plausible explanation for these differences. Furthermore, our results provide compelling support for our proposal that the increased ligand flexibility observed in Meta-I could lead to multiple retinal conformations in the active state (12).

Very few computational studies have been carried out on rhodopsin in the Meta-II state (18). This is the first attempt, to our knowledge, to use microscopic reversibility together with μs-long simulations to model the deactivation of rhodopsin. Our attempt to perturb this equilibrium starting from active Meta-II has led to the surprising discovery of a back-flip of retinal to an orientation found in the inactive photointermediates. The timescale of the flip occurs so quickly that it suggests the retinal binding pocket has evolved to stabilize the polyene chain in either of two conformations (i.e., up or down). In addition, these results provide compelling support for previous studies on GPCRs that identified loose coupling between agonist and protein upon activation (1,8; see Fig. S4 and Tables S1 and S2 in the Supporting Material). The role of the retinal flip in the interaction of transducin with rhodopsin, and the correspondence to other members of Class A GPCRs, remain as important questions for future research.

SUPPORTING MATERIAL

Supporting Materials and Methods, Supporting Discussion, six figures, four tables, and one movie are available at http://www.biophysj.org/biophysj/supplemental/S0006-3495(15)00459-2.

AUTHOR CONTRIBUTIONS

J.F. and B.M. designed research; J.F. performed research; J.F. and B.M. analyzed results; and J.F., M.F.B., and B.M. wrote the article.

ACKNOWLEDGMENTS

The authors thank M. Pitman, A. Struts, and T. Sakmar for discussions.

This work was supported by the National Institutes of Health (to M.F.B.) and West Virginia University (to B.M.). Computational time was provided through XSEDE allocation No. TG-MCB090200.

REFERENCES

1. Mahalingam, M., K. Martínez-Mayorga, …, R. Vogel. 2008. Two protonation switches control rhodopsin activation in membranes. *Proc. Natl. Acad. Sci. USA.* 105:17795–17800.
2. Standfuss, J., P. C. Edwards, …, G. F. X. Schertler. 2011. The structural basis of agonist-induced activation in constitutively active rhodopsin. *Nature.* 471:656–660.
3. Nakamichi, H., and T. Okada. 2006. Crystallographic analysis of primary visual photochemistry. *Angew. Chem. Int. Ed. Engl.* 45:4270–4273.
4. Palczewski, K., T. Kumasaka, …, M. Miyano. 2000. Crystal structure of rhodopsin: a G protein-coupled receptor. *Science.* 289:739–745.
5. Han, M., M. Groesbeek, …, S. O. Smith. 1997. The C9 methyl group of retinal interacts with glycine-121 in rhodopsin. *Proc. Natl. Acad. Sci. USA.* 94:13442–13447.
6. Deupi, X., P. Edwards, …, J. Standfuss. 2012. Stabilized G protein binding site in the structure of constitutively active metarhodopsin-II. *Proc. Natl. Acad. Sci. USA.* 109:119–124.
7. Choe, H.-W., Y. J. Kim, …, O. P. Ernst. 2011. Crystal structure of metarhodopsin II. *Nature.* 471:651–655.
8. Dror, R. O., D. H. Arlow, …, D. E. Shaw. 2011. Activation mechanism of the β_2-adrenergic receptor. *Proc. Natl. Acad. Sci. USA.* 108:18684–18689.

9. Deupi, X., and B. K. Kobilka. 2010. Energy landscapes as a tool to integrate GPCR structure, dynamics, and function. *Physiology (Bethesda).* 25:293–303.
10. Zaitseva, E., M. F. Brown, and R. Vogel. 2010. Sequential rearrangement of interhelical networks upon rhodopsin activation in membranes: the Meta II_a conformational substate. *J. Am. Chem. Soc.* 132:4815–4821.
11. Martínez-Mayorga, K., M. C. Pitman, …, M. F. Brown. 2006. Retinal counterion switch mechanism in vision evaluated by molecular simulations. *J. Am. Chem. Soc.* 128:16502–16503.
12. Leioatts, N., B. Mertz, …, M. F. Brown. 2014. Retinal ligand mobility explains internal hydration and reconciles active rhodopsin structures. *Biochemistry.* 53:376–385.
13. Zhu, S., M. F. Brown, and S. E. Feller. 2013. Retinal conformation governs pK_a of protonated Schiff base in rhodopsin activation. *J. Am. Chem. Soc.* 135:9391–9398.
14. Angel, T. E., S. Gupta, …, M. R. Chance. 2009. Structural waters define a functional channel mediating activation of the GPCR, rhodopsin. *Proc. Natl. Acad. Sci. USA.* 106:14367–14372.
15. Vogel, R., S. Lüdeke, …, M. Sheves. 2006. Agonists and partial agonists of rhodopsin: retinal polyene methylation affects receptor activation. *Biochemistry.* 45:1640–1652.
16. Deupi, X., and J. Standfuss. 2011. Structural insights into agonist-induced activation of G-protein-coupled receptors. *Curr. Opin. Struct. Biol.* 21:541–551.
17. Ahuja, S., E. Crocker, …, S. O. Smith. 2009. Location of the retinal chromophore in the activated state of rhodopsin. *J. Biol. Chem.* 284:10190–10201.
18. Rose, A. S., M. Elgeti, …, P. W. Hildebrand. 2014. Position of transmembrane helix 6 determines receptor G protein coupling specificity. *J. Am. Chem. Soc.* 136:11244–11247.

Supporting Material

Retinal Flip in Rhodopsin Activation?

Jun Feng,[1] Michael F. Brown,[2,3] and Blake Mertz[1]

[1]The C. Eugene Bennett Department of Chemistry, West Virginia University, Morgantown, West Virginia, USA. [2]Department of Chemistry and Biochemistry, University of Arizona, Tucson, Arizona, USA. [3]Department of Physics, University of Arizona, Tucson, Arizona, USA.

Contents:

Computational Methods

The initial structure of rhodopsin for the simulation was taken from the Meta-II state (PDB 3PXO). Crystal waters were retained for the simulation setup and no extra water molecules were added in the interior of protein. The principal axis of the protein was oriented parallel to the *z*-axis with the center of mass moved to the origin. To favor the reversible Meta-II to Meta-I back transition, the protonation states of amino acid residues were assigned according to the inactive Meta-I state. Specifically, residues Asp83$^{2.54}$ and Glu122$^{3.37}$ were protonated, and all other ionizable residues carried their standard charges at physiological pH (1). The all-*trans* ligand retinal was bound to Lys296$^{6.43}$ via a protonated Schiff base (15-*anti*). Both Glu113$^{3.28}$ and Glu181^{EL2} were deprotonated to reflect a complex counterion in the binding pocket, which has been verified experimentally by FTIR and solid-state ^{2}H NMR spectroscopy, and with MD simulations (2,3). In addition, Glu134$^{3.49}$, which undergoes cytoplasmic proton uptake only in the fully active Meta-II state, was deprotonated. To simulate the Meta-II state, Asp83$^{2.54}$, Glu113$^{3.28}$, and Glu122$^{3.37}$ were protonated, but the Schiff base was deprotonated. In all simulations, two palmitate molecules were covalently linked to Cys322^{CT} and Cys323^{CT}, respectively, with the aliphatic chains approximately parallel to the *z*-axis.

The replacement method of the Membrane Builder (4,5) from the CHARMM-GUI website (http://www.charmm-gui.org) was used to set up rhodopsin in an explicit hydrated lipid bilayer. To study the Meta-II to Meta-I state transition, three simulation systems were set up with different lipid bilayer compositions, i.e., DOPC/DOPE ratios of 3:1, 1:1, and 1:3, with 128 lipids in each leaflet (**Table S3**). One control simulation system was set up to favor the Meta-II state with a DOPC/DOPE ratio of 1:3. The protein and lipid bilayer were hydrated with at least 3 layers (~10 Å) of TIP3P water. Sodium and chloride ions were added to the simulation box to neutralize the system and maintain a salt concentration of 0.15 M. The final dimension of each system was approximately 100 Å × 100 Å × 95 Å.

All simulations were set up using CHARMM (6) and the MMTSB toolset (7) with the c36 CHARMM force field (8,9). The force field parameters of retinal were from Feller and coworkers (10,11). The simulations were initially run in NAMD (12) and then transferred using CHAMBER (13) to run in

AMBER12 (14) utilizing graphics processing unit (GPU) acceleration. All simulations were performed in the *NPT* ensemble. Langevin dynamics were used for temperature control at 300 K with a collision frequency of 5 ps^{-1}. Berendsen (15) non-isotropic pressure scaling with a relaxation time of 8 ps was employed for the membrane simulations. A timestep of 2 fs was used with bonds constrained with the SHAKE algorithm. Each trajectory was 3 μs long for a total of 12 μs simulation time. Coordinates were saved every 10 ps. Analysis was carried out using CHARMM (6), MDAnalysis (16), LOOS (17), and in-house scripts. Molecular visualization was done in VMD (18) and PyMOL (19).

Supplementary Table S1. Principal component analysis of retinal and rhodopsin in MD simulations.

Simulation	DOPC:DOPE	rhodopsin[a]			retinal		
		PC1[b]	PC2	PC3	PC1	PC2	PC3
Meta-II to Meta-I transition	3:1	36.12	11.78	6.48	75.76	6.03	4.67
	1:1	41.88	12.50	6.58	67.72	13.36	4.94
	1:3	27.00	10.56	8.20	64.09	14.03	4.71
Meta-II control	1:3	47.75	6.80	5.94	33.55	18.10	13.40

[a] Proportion (in percentage) of structural fluctuations captured by first, second, and third principal components (PC1, PC2, and PC3) in each simulation.

[b] Principal component analysis was applied to the C_α atoms of seven transmembrane helices (rhodopsin) and heavy atoms of retinal (retinal), respectively.

Supplementary Table S2. Correlation between first principal components of rhodopsin and retinal.

Simulation	lipid:lipid	$r_{\mathrm{RHO,RET}}$[a]
DOPC:DOPE	3:1	-0.76
DOPC:DOPE	1:1	0.70
DOPC:DOPE	1:3	-0.52
Meta-II	1:3	0.58

[a] The correlation between any other PC is negligible ($|r| \ll 0.3$).

Supplementary Table S3. Proteolipid systems modeled and details of each simulation.

simulation[a]	DOPC:DOPE[b]	lipid:protein[c]	# of atoms	retinal flip[b]	Glu113$^{3.28d}$	Glu134$^{3.49e}$	Schiff base[f]
Meta-II to Meta-I transition	3:1	256:1	94,789	yes	–	–	+
	1:1	256:1	94,405	no	–	–	+
	1:3	256:1	93,913	yes	–	–	+
Meta-II control	1:3	256:1	93,871	no	neutral	neutral	neutral

[a] All simulations started from Meta-II configuration (PDB ID 3PXO).
[b] Molar ratio.
[c] Yes = polyene chain underwent reorientation of the methyl groups towards the extracellular lid of rhodopsin.
[d] Counterion to the Schiff base and accepts proton from protonated Schiff base in the Meta-II state.
[e] Part of the conserved "ionic lock" in Class A GPCRs that undergoes proton uptake in Meta-II state.
[f] Covalent linkage between the retinal chromophore and the sidechain of Lys296$^{6.43}$, protonated until Meta-II state.

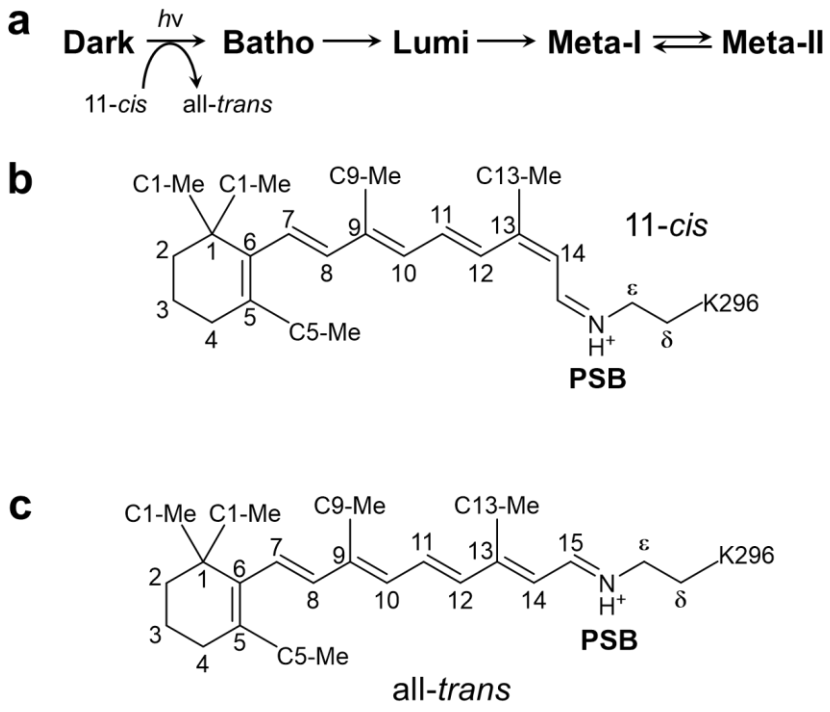

Supplementary Figure S1. Photocascade of rhodopsin is directly tied to action of the retinal chromophore. (a) The photocascade of rhodopsin. In the dark state, retinal is in the 11-*cis* conformation. Upon absorption of a photon, the retinal undergoes a *cis* to *trans* isomerization, facilitating the progression of rhodopsin through a series of photointermediates until it reaches equilibrium between the inactive Meta-I and active Meta-II states. 11-*cis* (b) and all-*trans* (c) forms of retinal. Note the protonated Schiff base (PSB) linkage to the side chain of Lys296$^{6.43}$.

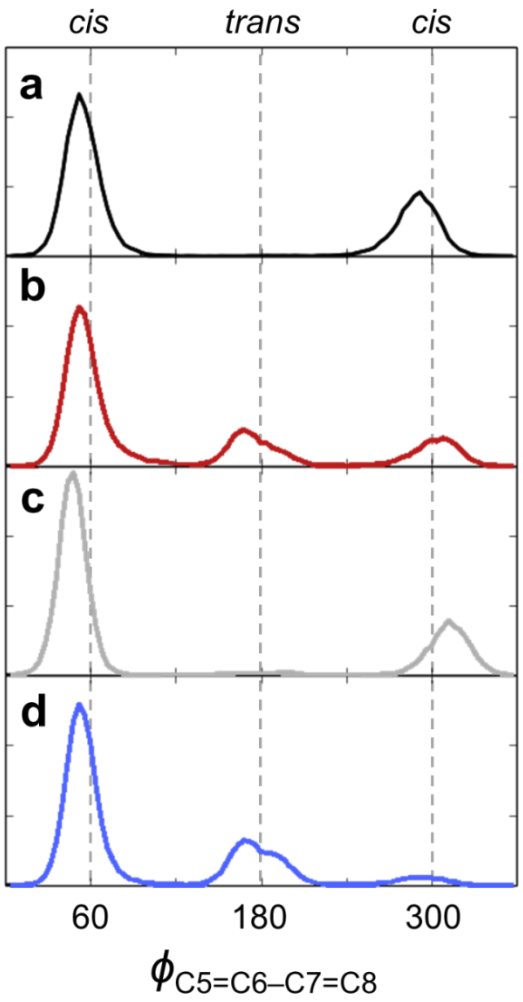

Supplementary Figure S2. The β-ionone ring of retinal can adopt both *cis* and *trans* conformations in the Meta-II state. Normalized distribution of the C5=C6–C7=C8 dihedral angle between the β-ionone ring and the polyene chain of retinal. When the retinal polyene chain methyl groups are oriented towards the cytoplasmic side of the protein, the β-ionone ring fluctuates between 6-*s*-*cis* conformations (60 and 300 deg, respectively). However, after a flip of the polyene chain and orientation toward the extracellular lid, the β-ionone ring adopts a 6-*s*-*trans* conformation (180 deg). (a) Rhodopsin in the Meta-II protonation states embedded in a DOPC:DOPE (3:1 molar ratio) bilayer, (b) rhodopsin in the Meta-I protonation states embedded in a DOPC:DOPE (1:3) bilayer, (c) rhodopsin (Meta-I) in a DOPC:DOPE (1:1) bilayer, and (d) rhodopsin (Meta-I) in a DOPC:DOPE (3:1) bilayer.

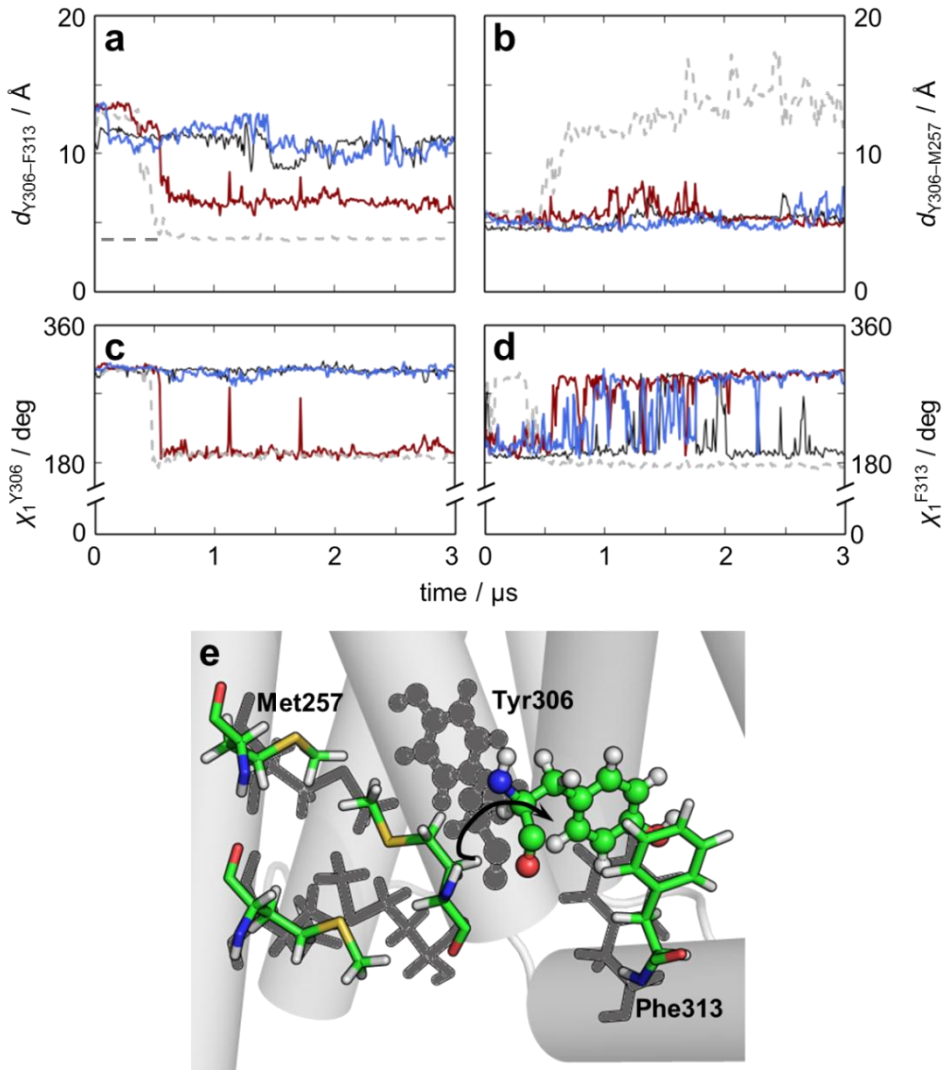

Supplementary Figure S3. The NPxxY motif fluctuates between active and inactive conformations during molecular (MD) simulations. (a) Stabilizing aromatic stacking interactions are reestablished between Tyr306$^{7.53}$ and Phe313$^{7.60}$ in two of the DOPC:DOPE simulations; *black*: Meta-II; *blue*: DOPC/DOPE (3:1); *gray*: DOPC/DOPE (1:1); *red*: DOPC/DOPE (1:3). (b) Breaking of interactions between Tyr306$^{7.53}$ and Met257$^{6.40}$ is not always required. (c) Reestablishment of stacking interactions is due to rotation of Tyr306$^{7.53}$ around the χ_1 dihedral but (d) not χ_1 of Phe313$^{7.60}$. (e) Representative snapshots from MD trajectories show that the NPxxY motif has several modes of nonbonded interactions between interleaved methionine sidechains in TM6 and TM7 (gray outline: DOPC/DOPE (3:1); green: DOPC/DOPE (1:1)).

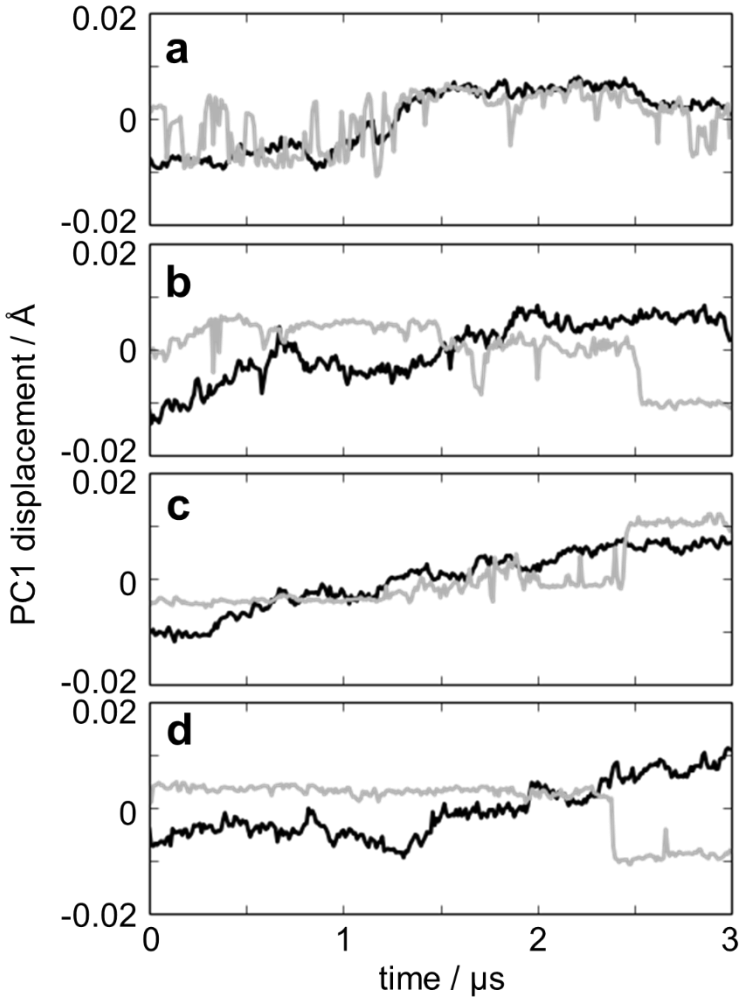

Supplementary Figure S4. Time evolution of the first principal components of retinal and rhodopsin. PC1s are shown for retinal (*gray*) and rhodopsin (*black*) over the course of the MD simulations, demonstrating loose coupling between the two components. (a) Meta-II, (b) DOPC:DOPE (1:3), (c) DOPC:DOPE (1:1), (d) DOPC:DOPE (3:1).

Supplementary discussion

After verifying the stability of our system and that it reproduces the lipid bilayer properties (**Table S4** and **Fig. S5**), we examined characteristics that are structural hallmarks for the transition of rhodopsin from the Meta-II to the Meta-I state. Rearrangements of key amino acid side chains within the retinal binding pocket that facilitate the transition to the active Meta-II state, such as Ile189^{EL2}, Tyr191^{EL2}, Trp265$^{6.47}$, and Tyr268$^{6.51}$ (20), are intimately involved with the retinal cofactor. In addition to the stabilizing interactions with the C9-methyl group, Tyr191^{EL2} also stabilizes the C13-methyl group (**Fig. S6**). However, the majority of binding pocket interactions that are notably different between crystallographic (21) and NMR (22) studies are stable, regardless of the retinal flip. These rearrangements of side chains parallel to the long axis of the polyene chain contribute to the stabilization of retinal oriented towards the extracellular lid of rhodopsin for the remainder of the simulation (~500 ns). Moreover, the region surrounding the β-ionone ring is surprisingly stable, providing an environmental context to the quantum chemical studies conducted *in vacuo* that recently identified a direct correlation between the C5=C6–C7=C8 dihedral and the pK_a of the Schiff base (10). These studies showed that the SB possessed a pK_a favorable to deprotonation (< 7) when the β-ionone ring was in a twisted 6-*s*-*cis* conformation, whereas a 6-*s*-*trans* conformation favored a protonated SB (> 9). It appears that the energy barrier is greater for rotation of the β-ionone ring rather than the polyene chain, contrary to what had been shown for rhodopsin in the dark state (23). Nevertheless, our results agree with the original hypothesis that the β-ionone ring can sample multiple conformations (*cis* or *trans*) (**Fig. S2**), which in our case is due to fluctuations of the polyene chain, rather than the ionone ring.

Another important aspect is that hydration of the protein interior changes during rhodopsin activation, although it has been difficult to characterize (24). Our MD simulations (25) as well as crystal structures (26) have identified a possible water channel that connects the cytoplasmic side of the protein with the retinal binding pocket. Together with the helical tilt of TM5 and outward rotation of TM6 in the active state (27), there is evidence for an increase in the internal protein volume that is accessible to bulk solution. By contrast, several studies have postulated that the Meta-II state is accessible only *via*

dehydration (28,29), which has led to conflicting views on the role of water flux in rhodopsin activation. Our results tend to favor the former view; it is conceivable that with longer timescales, we could potentially observe larger-scale conformational changes in the TM helical bundle that could shed more light on this critical issue.

Previous long-timescale MD simulation studies conducted on the β_2-adrenergic receptor revealed loose coupling between the movements of the agonist binding pocket, the G protein binding site, and a connector region that links the two (30). Since rhodopsin is a Class A GPRCR like the β_2-adrenergic receptor, it would be highly relevant to see if the motions of retinal acting as an agonist in the Meta-II state have a similar effect on the overall motions of the protein. We conducted principal component analysis (PCA) of the retinal chromophore and the apo form of rhodopsin in order to determine the dominant motions over the course of our simulations. Our results show that the first principal component (PC1) captures the majority of the retinal fluctuations in each of the DOPC/DOPE simulations, but not in the Meta-II simulation (**Table S1**). PC1 of the protein is less dominant in all simulations, capturing less than half of the structural fluctuations, indicating that the motions of rhodopsin are much more complex than the chromophore.

To assess the relationship between principal components (PCs) of the retinal and rhodopsin, we calculated the correlation coefficient among first ten PCs, $r\left(\mathrm{PC}_i^{\mathrm{RHO}}, \mathrm{PC}_j^{\mathrm{RET}}\right)$ for $1 \leq i, j \leq 10$. The results reveal that the motions of the retinal and rhodopsin are not strongly correlated (**Table S2**), and this can also be seen in the time evolution of PC1 for retinal and rhodopsin (**Fig. S3**). This finding appears to support the hypothesis suggested by Dror and coworkers that identified loose coupling between agonist binding and conformational changes within the G protein binding site on the cytoplasmic side of the β_2-adrenergic receptor (30). However, further investigation in our rhodopsin systems and in other GPCR systems is necessary in order to more fully understand this structural behavior.

Supplementary Table S4. Area per lipid at aqueous interface.

Simulation[a,b]	lipid:lipid[c]	Area per Lipid[c,d] / Å^2
Meta-II	3:1	61.2±0.7
1DOPC:3DOPE	1:1	61.6±0.9
1DOPC:1DOPE	1:3	62.9±0.9
3DOPC:1DOPE	1:3	64.6±0.9

[a] Calculated from trajectory after 0.5 μs.
[b] Protein cross-sectional area estimated to be 1242 Å^2.
[c] Molar ratio
[d] Values of surface area per lipid from pure DOPC system using CHARMM c36 force field at 303 K is 69.0±0.3 Å^2.[1]
[e] Experimental values of surface area per lipid are 67.4±1.0 Å^2 for DOPC at 303 K (31) and 60 Å^2 for DOPE at 271 K (32).

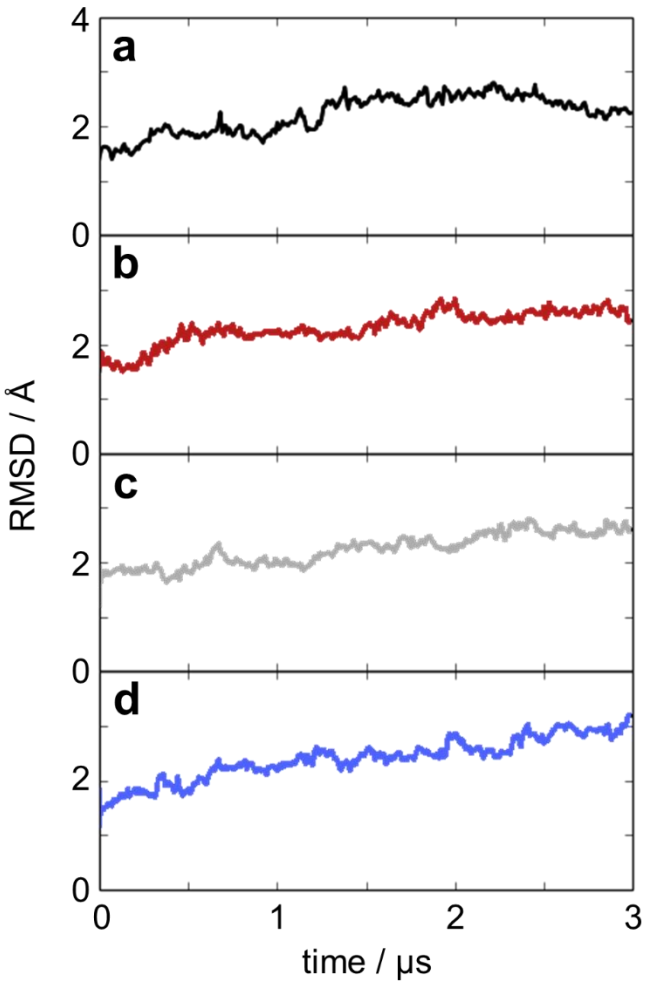

Supplementary Figure S5. Heavy-atom root-mean-square-deviation (RMSD) of seven transmembrane helices from Meta II crystal structure. RMSDs were calculated in order to verify stability of the heptahelical bundle over microsecond timescales. (a) Meta-II, (b) DOPC:DOPE (1:3), (c) DOPC:DOPE (1:1), (d) DOPC:DOPE (3:1).

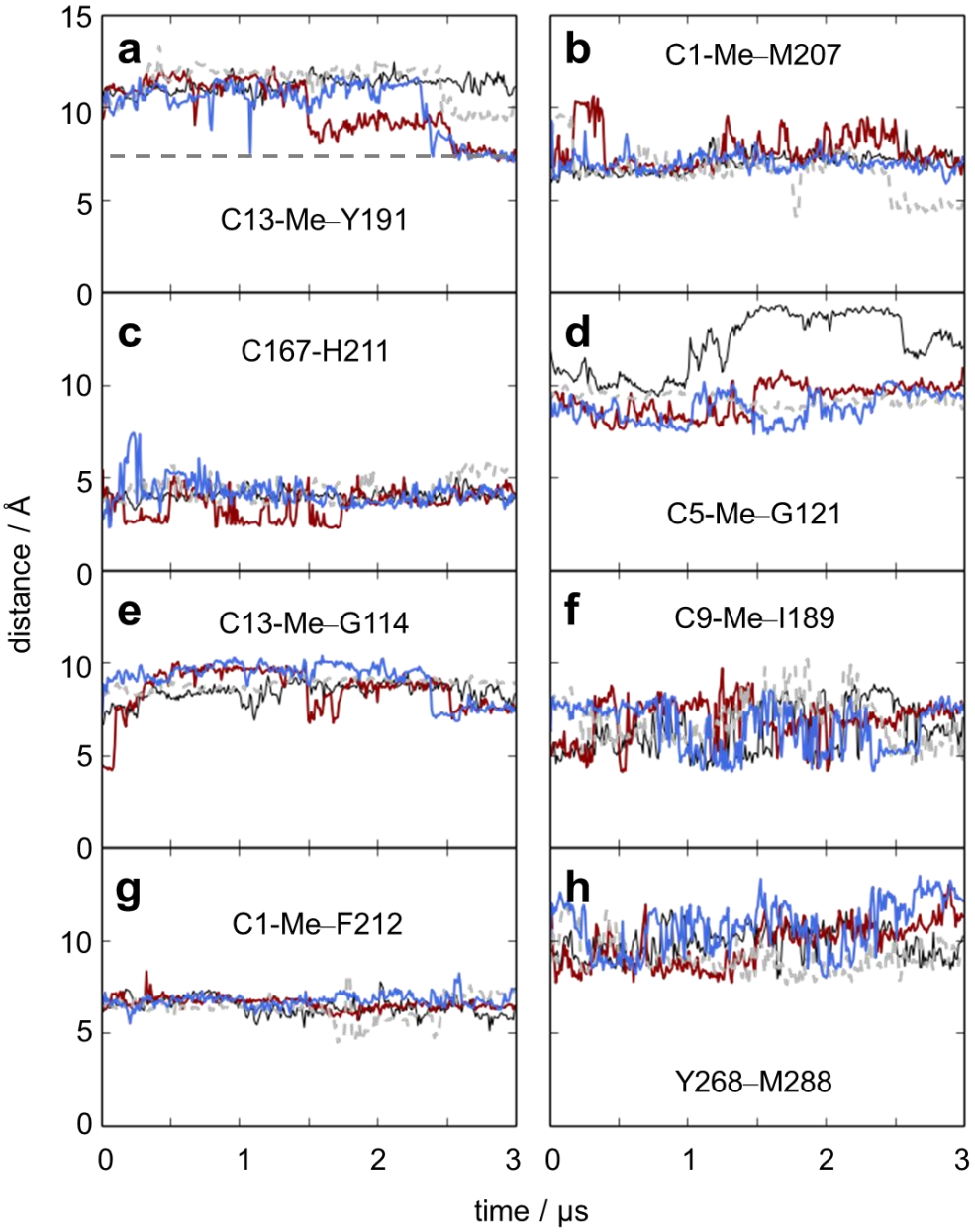

Supplementary Figure S6. Retinal binding pocket stabilizes the retinal polyene chain in two different orientations. After the retinal flip, interactions between the C13-methyl and Tyr191^{EL2} are restored (a). However, the majority of binding pocket interactions that are notably different between crystallographic (21) and NMR studies (22) are stable regardless of the retinal orientation (b-h).

Supplementary Movie S1. Flip of retinal in the binding pocket. Time evolution from the DOPC:DOPE (3:1) trajectory in which the polyene chain flips from the cytoplasmic side of the protein and Trp265$^{6.48}$ (bottom) towards the extracellular lid of the protein and Tyr191^{EL2} (top). Note the two-state conformation of the polyene chain ("down" to "up") and the fluctuation of the Trp265$^{6.48}$ χ_1 dihedral (part of the "transmission switch" (33)).

Supporting References

1. Periole, X., M.A. Ceruso, and E.L. Mehler. 2004. Acid−Base Equilibria in Rhodopsin: Dependence of the Protonation State of Glu134 on Its Environment. Biochemistry 43: 6858–6864.

2. Ludeke, S., M. Beck, E.C.Y. Yan, T.P. Sakmar, F. Siebert, and R. Vogel. 2005. The Role of Glu181 in the Photoactivation of Rhodopsin. J. Mol. Biol. 353: 345–356.

3. Martinez-Mayorga, K., M.C. Pitman, A. Grossfield, S.E. Feller, and M.F. Brown. 2006. Retinal Counterion Switch Mechanism in Vision Evaluated by Molecular Simulations. J. Am. Chem. Soc. 128: 16502–16503.

4. Jo, S., T. Kim, and W. Im. 2007. Automated Builder and Database of Protein/Membrane Complexes for Molecular Dynamics Simulations. PLoS ONE. 2: e880.

5. Jo, S., J.B. Lim, J.B. Klauda, and W. Im. 2009. CHARMM-GUI Membrane Builder for Mixed Bilayers and Its Application to Yeast Membranes. Biophys. J. 97: 50–58.

6. Brooks, B.R., C.L. Brooks, A.D. Mackerell, L. Nilsson, R.J. Petrella, B. Roux, Y. Won, G. Archontis, C. Bartels, S. Boresch, A. Caflisch, L. Caves, Q. Cui, A.R. Dinner, M. Feig, S. Fischer, J. Gao, M. Hodoscek, W. Im, K. Kuczera, T. Lazaridis, J. Ma, V. Ovchinnikov, E. Paci, R.W. Pastor, C.B. Post, J.Z. Pu, M. Schaefer, B. Tidor, R.M. Venable, H.L. Woodcock, X. Wu, W. Yang, D.M. York, and M. Karplus. 2009. CHARMM: The biomolecular simulation program. J. Comput. Chem. 30: 1545–1614.

7. Feig, M., J. Karanicolas, and C.L. Brooks III. 2004. MMTSB Tool Set: enhanced sampling and multiscale modeling methods for applications in structural biology. J. Mol. Graph. Model. 22: 377–395.

8. Klauda, J.B., V. Monje, T. Kim, and W. Im. 2012. Improving the CHARMM Force Field for Polyunsaturated Fatty Acid Chains. J. Phys. Chem. B. 116: 9424–9431.

9. Best, R.B., X. Zhu, J. Shim, P.E.M. Lopes, J. Mittal, M. Feig, and A.D. MacKerell. 2012. Optimization of the Additive CHARMM All-Atom Protein Force Field Targeting Improved Sampling of the Backbone ϕ, ψ and Side-Chain χ1 and χ2 Dihedral Angles. J. Chem. Theory Comput. 8: 3257–3273.

10. Zhu, S., M.F. Brown, and S.E. Feller. 2013. Retinal Conformation Governs pKa of Protonated Schiff Base in Rhodopsin Activation. J. Am. Chem. Soc. 135: 9391–9398.

11. Mertz, B., M. Lu, M.F. Brown, and S.E. Feller. 2011. Steric and electronic influences on the torsional energy landscape of retinal. Biophys. J. 101: L17–19.

12. Phillips, J.C., R. Braun, W. Wang, J. Gumbart, E. Tajkhorshid, E. Villa, C. Chipot, R.D. Skeel, L. Kalé, and K. Schulten. 2005. Scalable molecular dynamics with NAMD. J. Comput. Chem. 26: 1781–1802.

13. Crowley, M.F., M.J. Williamson, and R.C. Walker. 2009. CHAMBER: Comprehensive support for CHARMM force fields within the AMBER software. Int. J. Quantum Chem. 109: 3767–3772.

14. Case, D.A., T.A. Darden, T.E. Cheatham III, C.L. Simmerling, J. Wang, R.E. Duke, R. Luo, R.C. Walker, W. Zhang, K.M. Merz, B. Roberts, S. Hayik, A. Roitberg, G. Seabra, J. Swails, A.W. Goetz, I. Kolossvary, K.F. Wong, F. Paesani, J. Vanicek, R.M. Wolf, J. Liu, X. Wu, S.R. Brozell, T. Steinbrecher, H. Gohlke, Q. Cai, X. Ye, J. Wang, M.-J. Hsieh, G. Cui, D.R. Roe, D.H. Mathews, M.G. Seetin, R. Salomón-Ferrer, C. Sagui, V. Babin, T. Luchko, S. Gusarov, A. Kovalenko, and P.A. Kollman. 2012. Amber 12. University of California, San Francisco.

15. Berendsen, H.J.C., J.P.M. Postma, W.F. van Gunsteren, A. DiNola, and J.R. Haak. 1984. Molecular dynamics with coupling to an external bath. J. Chem. Phys. 81: 3684–3690.

16. Michaud-Agrawal, N., E.J. Denning, T.B. Woolf, and O. Beckstein. 2011. MDAnalysis: A toolkit for the analysis of molecular dynamics simulations. J. Comput. Chem. 32: 2319–2327.

17. Romo, T.D., N. Leioatts, and A. Grossfield. 2014. Lightweight object oriented structure analysis: Tools for building tools to analyze molecular dynamics simulations. J. Comput. Chem. 35: 2305–2318.

18. Humphrey, W., A. Dalke, and K. Schulten. 1996. VMD: visual molecular dynamics. J. Mol. Graph. 14: 33–38, 27–28.

19. The PyMOL Molecular Graphics System, Version 1.7.0. Schrödinger, LLC.

20. Vogel, R., S. Lüdeke, F. Siebert, T.P. Sakmar, A. Hirshfeld, and M. Sheves. 2006. Agonists and partial agonists of rhodopsin: retinal polyene methylation affects receptor activation. Biochemistry 45: 1640–1652.

21. Choe, H.-W., Y.J. Kim, J.H. Park, T. Morizumi, E.F. Pai, N. Krausz, K.P. Hofmann, P. Scheerer, and O.P. Ernst. 2011. Crystal structure of metarhodopsin II. Nature. 471: 651–655.

22. Ahuja, S., E. Crocker, M. Eilers, V. Hornak, A. Hirshfeld, M. Ziliox, N. Syrett, P.J. Reeves, H.G. Khorana, M. Sheves, and S.O. Smith. 2009. Location of the retinal chromophore in the activated state of rhodopsin. J. Biol. Chem. 284: 10190–10201.

23. Lau, P.-W., A. Grossfield, S.E. Feller, M.C. Pitman, and M.F. Brown. 2007. Dynamic Structure of Retinylidene Ligand of Rhodopsin Probed by Molecular Simulations. J. Mol. Biol. 372: 906–917.

24. Jastrzebska, B., K. Palczewski, and M. Golczak. 2011. Role of bulk water in hydrolysis of the rhodopsin chromophore. J. Biol. Chem. 286: 18930–18937.

25. Leioatts, N., B. Mertz, K. Martínez-Mayorga, T.D. Romo, M.C. Pitman, S.E. Feller, A. Grossfield, and M.F. Brown. 2014. Retinal ligand mobility explains internal hydration and reconciles active rhodopsin structures. Biochemistry 53: 376–385.

26. Angel, T.E., S. Gupta, B. Jastrzebska, K. Palczewski, and M.R. Chance. 2009. Structural waters define a functional channel mediating activation of the GPCR, rhodopsin. Proc. Natl. Acad. Sci. U. S. A. 106: 14367–14372.

27. Altenbach, C., A.K. Kusnetzow, O.P. Ernst, K.P. Hofmann, and W.L. Hubbell. 2008. High-resolution distance mapping in rhodopsin reveals the pattern of helix movement due to activation. Proc. Natl. Acad. Sci. U. S. A. 105: 7439–44.

28. Mitchell, D.C., and B.J. Litman. 1999. Effect of Protein Hydration on Receptor Conformation: Decreased Levels of Bound Water Promote Metarhodopsin II Formation. Biochemistry 38: 7617–7623.

29. Mitchell, D.C., and B.J. Litman. 2000. Effect of Ethanol and Osmotic Stress on Receptor Conformation. Reduced Water Activity Amplifies the Effect of Ethnol on Metarhodopsin II Formation. J. Biol. Chem. 275: 5355–5360.

30. Dror, R.O., D.H. Arlow, P. Maragakis, T.J. Mildorf, A.C. Pan, H. Xu, D.W. Borhani, and D.E. Shaw. 2011. Activation mechanism of the β 2-adrenergic receptor. Proc. Natl. Acad. Sci. U. S. A. 108: 18684–18689.

31. Klauda, J.B., R.M. Venable, J.A. Freites, J.W. O'Connor, D.J. Tobias, C. Mondragon-Ramirez, I. Vorobyov, A.D. MacKerell, and R.W. Pastor. 2010. Update of the CHARMM All-Atom Additive Force Field for Lipids: Validation on Six Lipid Types. J. Phys. Chem. B. 114: 7830–7843.

32. Gawrisch, K., V.A. Parsegian, D.A. Hajduk, M.W. Tate, S.M. Gruner, N.L. Fuller, and R.P. Rand. 1992. Energetics of a hexagonal-lamellar-hexagonal-phase transition sequence in dioleoylphosphatidylethanolamine membranes. Biochemistry 31: 2856–2864.

33. Deupi, X., and J. Standfuss. 2011. Structural insights into agonist-induced activation of G-protein-coupled receptors. Curr. Opin. Struct. Biol. 21: 541–551.